Published OnlineFirst July 2, 2018; DOI: 10.1158/0008-5472.CAN-18-1126

Convergence and Technologies

Cancer Research

High-Throughput Screening of Combinatorial Immunotherapies with Patient-Specific *In Silico* Models of Metastatic Colorectal Cancer

Jakob Nikolas Kather[1,2,3], Pornpimol Charoentong[1,3], Meggy Suarez-Carmona[1,3], Esther Herpel[4,5], Fee Klupp[6], Alexis Ulrich[6], Martin Schneider[6], Inka Zoernig[1,3], Tom Luedde[7], Dirk Jaeger[1,2,3], Jan Poleszczuk[8], and Niels Halama[1,2,3]

Abstract

Solid tumors are rich ecosystems of numerous different cell types whose interactions lead to immune escape and resistance to immunotherapy in virtually all patients with metastatic cancer. Here, we have developed a 3D model of human solid tumor tissue that includes tumor cells, fibroblasts, and myeloid and lymphoid immune cells and can represent over a million cells over clinically relevant timeframes. This model accurately reproduced key features of the tissue architecture of human colorectal cancer and could be informed by individual patient data, yielding *in silico* tumor explants. Stratification of growth kinetics of these explants corresponded to significantly different overall survival in a cohort of patients with metastatic colorectal cancer. We used the model to simulate the effect of chemotherapy, immunotherapies, and cell migration inhibitors alone and in combination. We classified tumors according to tumor and host characteristics, showing that optimal treatment strategies markedly differed between these classes. This platform can complement other patient-specific *ex vivo* models and can be used for high-throughput screening of combinatorial immunotherapies.

Significance: This patient-informed *in silico* tumor growth model allows testing of different cancer treatment strategies and immunotherapies on a cell/tissue level in a clinically relevant scenario. *Cancer Res; 78(17); 5155–63. ©2018 AACR.*

Introduction

Gastrointestinal solid tumors such as colorectal cancer account for a significant burden of morbidity and mortality. Despite many efforts, microsatellite-stable colorectal cancer, the most common type of this disease, is resistant to all approved immunotherapy approaches (1). A main reason for this is the immunosuppressive effect of the tumor microenvironment (TME), with abundant stroma, many protumor macrophages and few tumor-infiltrating lymphocytes. Together with tumor cells, these cells form a complex ecosystem with emergent properties that lead to immune escape and immunotherapy resistance.

Cancer immunotherapy alone or in combination can, in principle, overcome these immunosuppressive adaptations, with combinational treatment being currently regarded as the most promising approach (2). However, given the large number of approved and candidate drugs, it is not feasible to compare all immunotherapy agents in a clinical setting. Rather, various experimental *ex vivo* models are used to study combination treatment effects on tumors, among them classical cell culture models, tumor organoids (3), and patient-derived xenografts (PDX; refs. 4–6).

Most of these models suffer from limited scalability and do not fully recapitulate the complex cellular interactions in the TME. In principle, computer-based (*in silico*) models of tumor growth can address these shortcomings as they can be designed to incorporate various cellular interactions, can be arbitrarily scaled, and can be informed by individual patient data, constituting *in silico* patient-derived tumor explants (7). However, until now, no such model has been available. Previous 3D spatial models of human solid tumors have reflected some aspects of realistic phenotypes. However, these models have not explicitly included lymphocytes, stroma, and macrophages (8, 9), which are key players in colorectal cancer (10), or have incorporated some parts of the microenvironment without clinical validation and in a computationally expensive way (11). To our knowledge, there is currently no computational model of tumor growth that encompasses all relevant aspects of the TME and, at the same time, runs fast enough to be fitted to clinicopathologic data on a per-patient basis in thousands of model runs, which is a requirement for drug screening and other clinically relevant applications.

[1]Department of Medical Oncology and Internal Medicine VI, National Center for Tumor Diseases, University Hospital Heidelberg, Heidelberg, Germany. [2]German Cancer Consortium (DKTK), Heidelberg, Germany. [3]Applied Tumor Immunity, German Cancer Research Center (DKFZ), Heidelberg, Germany. [4]Institute of Pathology, Heidelberg University, Heidelberg, Germany. [5]Tissue Bank of the National Center for Tumor Diseases (NCT), Heidelberg, Germany. [6]Department of Surgery, University Hospital Heidelberg, Heidelberg, Germany. [7]Division of Gastroenterology, Hepatology and Hepatobiliary Oncology, University Hospital RWTH Aachen, Aachen, Germany. [8]Nalecz Institute of Biocybernetics and Biomedical Engineering, Polish Academy of Sciences, Warsaw, Poland.

Note: Supplementary data for this article are available at Cancer Research Online (http://cancerres.aacrjournals.org/).

J. Poleszczuk and N. Halama jointly supervised this work.

Corresponding Authors: Jakob Nikolas Kather, National Center for Tumor Diseases, University Medical Center Heidelberg, Im Neuenheimer Feld 460, 69120 Heidelberg, Germany. Phone: 49-6221-567229; Fax: 49-6221-567225; E-mail: jakob.kather@nct-heidelberg.de, and Niels Halama, E-mail: niels.halama@nct-heidelberg.de

doi: 10.1158/0008-5472.CAN-18-1126

Published OnlineFirst July 2, 2018; DOI: 10.1158/0008-5472.CAN-18-1126

In the present study, we designed a computationally efficient, three-dimensional agent-based *in silico* model of human colorectal cancer. This model includes tumor cells, lymphocytes, macrophages, fibrotic stroma, and necrosis, can grow large tumors of $>10^6$ cells in a few minutes on standard computer hardware. The model can be fitted to individual patient data and can be used for high-throughput screening of combination immunotherapies. To our knowledge, this is the first personalized *in silico* model of colorectal cancer with potential direct applicability in the clinic.

Materials and Methods

Ethics statement

All experiments were conducted in accordance with the Declaration of Helsinki, the International Ethical Guidelines for Biomedical Research Involving Human Subjects (CIOMS), the Belmont Report, and the US Common Rule. We used archival formalin-fixed paraffin-embedded material of human colorectal cancer liver metastases. All tissue samples were provided by the tissue bank of the National Center for Tumor Diseases (NCT, Heidelberg, Germany) in accordance with the regulations of the tissue bank and the approval of the ethics committee of Heidelberg University (S-207/2005, renewed on December 20, 2017, tissue bank decision number 2152, granted to N. Halama and J.N. Kather). We obtained written informed consent from all patients as part of the NCT biobank standard operating procedures. Also, correctness of the original pathology report was validated as part of the NCT biobank protocol. No cell culture experiments were performed as part of this study.

Digital pathology tissue analysis

$CD8^+$ cell fraction and $CD68^+$ cell fraction were quantified in immunostained serial sections of colorectal cancer liver metastasis tissue. QuPath version 0.1.2 (12, 13) was used to detect and classify cells in a representative, manually defined region of interest (ROI) of 1 mm width from the tumor–liver interface toward the tumor core, excluding artifacts and necrotic areas. Stroma–tumor ratio was also determined in ROIs drawn with similar criteria and areas of desmoplastic stroma were manually delineated by histomorphologic aspect in hematoxylin-stained sections using the wand tool by a trained observer. All analyses were conducted in a blinded fashion. All measurements are given as mean $\pm$ standard deviation unless otherwise noted.

Model design and implementation

We developed an on-grid, three-dimensional (3D) stem-cell–driven (14) agent-based model (Fig. 1A). As a blueprint for a complex agent-based model of the human colorectal cancer microenvironment, we used a well-characterized model from our recent study (15). That previous model contained only tumor cells, active and exhausted lymphocytes, stroma, and necrosis. In the present study, we added naïve macrophages and protumor macrophages to the model, markedly increasing the model's complexity (Fig. 1B). Our assumptions of these populations in the model are the following: nonpolarized (naïve) macrophages are just bystanders and do not exert relevant effects on lymphocyte function, but can polarize and become protumor macrophages. These protumor macrophages locally inhibit lymphocyte action as we have previously shown experimentally (10). Lymphocyte inhibition via protumor macrophages was attained via the concept of adjuvanticity (see below). Macrophage polarization probability was deduced from Koelzer and colleagues (16). With T lymphocytes and macrophages in different functional states, this model included key players that orchestrate the TME (10). Furthermore, we added the notion of adjuvanticity and antigenicity, which are both prerequisites for tumor cell killing by lymphocytes (17).

Regarding antigenicity, we considered that tumor cells have a fixed probability of acquiring an immunogenic mutation during cell division. As long as the number of immunogenic mutations in a given tumor cell is below a certain threshold, lymphocytes cannot attack that tumor cell. The number of mutations is inherited by daughter cells and, consequently, macroscopic tumors in our simulation are a heterogeneous mixture of tumor cell clones with different antigenicity. This notion is in accordance with previous models and experimental observation of tumor cell clonality in human tumors (18–20).

Besides antigenicity, we assumed that lymphocyte attacks on tumor cells also require signals from the microenvironment. We implemented this as an "adjuvanticity map," which stored the "adjuvanticity level" for each location on the lattice. In real tumors, there is a multitude of these signals. For the purposes of this model and in accordance with the literature, we refer to the sum of these signals as "adjuvanticity" (1, 17). To keep the model as simple as possible as well as biologically grounded, we assumed only one positive signal and one negative signal. We assumed that dying tumor cells would release small amounts of immunostimulatory molecules such as danger-associated molecular patterns that accumulate locally and increase local adjuvanticity. Conversely, protumor macrophages would release small amounts of inhibitory molecules that would locally decrease adjuvanticity. Although a multitude of factors might contribute to adjuvanticity in biological systems, we considered these two main factors in the model, as they have been empirically shown to be of utmost importance in metastatic colorectal cancer (1). Lastly, we expanded the model from 2D to 3D, increasing the number of cells that can be simulated by two orders of magnitude to approximately 10^6 cells. More details on the model design and implementation are available in the Supplementary Methods.

Figure 1C–F shows four examples of tumors that were simulated with the modeling platform, all of which are on a clinically relevant scale of several millimeters. Tumors in Fig. 1E and F contained approximately 10^6 cells, but computation time was still below 10 minutes (below 1 minute in case of parallel processing with 24 cores). All experiments were done in Matlab R2017b. The core of the simulation platform was developed in C++ using Eigen template library for linear algebra and SuiteSparse, which is a suite of sparse matrix algorithms and was interfaced with the Matlab program via MEX. Along with the core model, we implemented several types of visualization that allow for real-time monitoring of all crucial features of the model during tumor simulation (Supplementary Fig. S1A–S1E).

Code availability

All source codes are freely available under an open source license (DOI 10.5281/zenodo.1248806), allowing the simulations to be reproduced, applied to other datasets, and extended to other clinical scenarios and other tumor types, including primary tumors. Details on the parametrization are provided in Supplementary Methods and shown in Supplementary Fig. S2A and S2B.

Parameter fitting

We performed three rounds of model fitting using particle swarm optimization (PSO, details are given in Supplementary

Published OnlineFirst July 2, 2018; DOI: 10.1158/0008-5472.CAN-18-1126

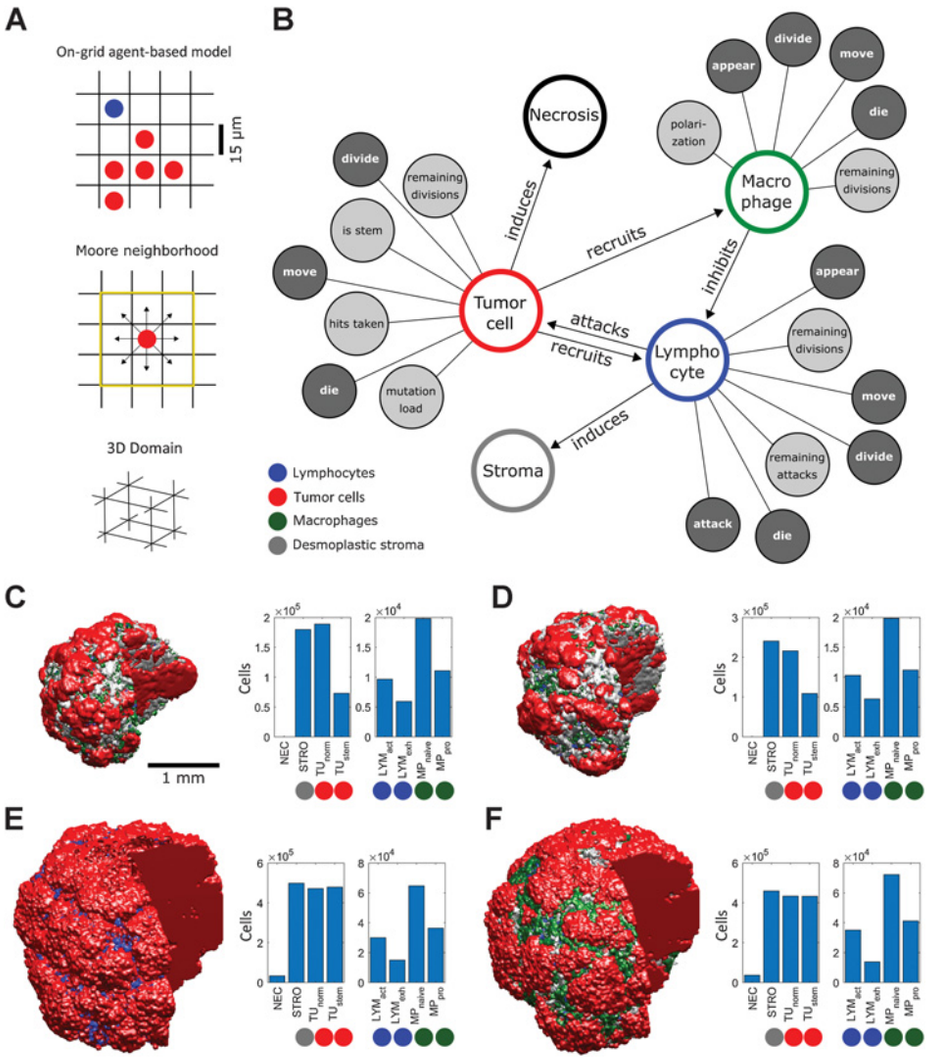

Figure 1.
An agent-based model of the colorectal cancer microenvironment. **A,** We implemented an on-grid, 3D agent-based model with Moore neighborhood. **B,** The agent-based model contains three types of players, tumor cells, lymphocytes, and macrophages, each of whom has a set of properties (bright gray circles) and abilities (dark gray circles). Also, two environmental features are modeled, fibrotic (desmoplastic) stroma and necrosis. Macrophages inhibit lymphocyte function in their vicinity (as shown in ref. 10); lymphocytes migrate toward tumor cells and can attack them (as shown in ref. 15). High tumor cell density induces necrosis and lymphocytes seed fibrotic stroma. **C–F,** Simulation of four tumors on a millimeter scale, comprising up to 10^6 cells. NEC, necrosis; STRO, desmoplastic stroma; TUnorm, normal tumor cell; TUstem, tumor stem cell; LYMact, active lymphocyte; LYMexh, exhausted lymphocyte; MPnaive, naïve macrophage; MPpro, protumor macrophage.

Methods). All model parameters are listed in Supplementary Table S1.

Fitting to population-based data. We fitted the model to five target variables. First, from our own quantitative histologic data sets ($N = 14$ colorectal cancer liver metastases stained with H&E, anti-CD8, and anti-CD68 as described before; ref. 10), we derived three target variables (Supplementary Table S2): (i) lymphocyte–tumor ratio (0.0332 ± 0.0411), (ii) macrophage–tumor ratio (0.0978 ± 0.0825), (iii) stroma–tumor ratio (0.2263 ± 0.1562). Furthermore, we used (iv) exhausted lymphocyte fraction (0.366 ± 0.157) derived from (21) and (v) tumor stem cell fraction (0.25) approximated from (22), assuming as standard deviation of 0.2. The loss function was defined as the root mean square error of these components normalized to their respective standard deviation. Using PSO, it was possible to fit the model to this loss function with a loss of <0.2 in repeated runs, indicating a very good fit. Thus, we conclude that the model can be successfully fit to real-world observations.

Patient-specific fitting. In total, 24 colorectal adenocarcinoma liver metastases with overall survival data (9-year follow-up; Supplementary Table S3) were provided by the NCT biobank as described before (23). We used PSO to fit the model to a loss function containing macrophage/lymphocyte/stroma-to-tumor ratio, assuming a standard deviation of 25% for these measurement values (Supplementary Fig. S3; Supplementary Table S4). After obtaining a six-dimensional parameter vector for each patient by PSO, we used these parameter sets to simulate macroscopic tumors. We then assessed the tumor growth rate $g = (T_{60} - T_{45})/T_{45}$, with T_n being the tumor cell number at day n (Supplementary Table S5). Patients were then stratified in two groups according to this relative tumor growth (growth speed, splitting at the median) and overall survival (OS) statistics were assessed using R software (R-project.org) using the packages "survminer" and "survival"; "survdiff" was used to calculate a P value with the log-rank test.

Fitting to different scenarios of adjuvanticity and antigenicity. We varied the fraction of tumor cells in low-antigenicity and

Published OnlineFirst July 2, 2018; DOI: 10.1158/0008-5472.CAN-18-1126

low-adjuvanticity conditions with three levels (high, mid, and low) as shown in Supplementary Table S6, yielding nine combinations. We used these conditions in a loss function and used PSO to fit the six free parameters to these conditions. Thereby, we obtained nine sets of six parameters, each of which could be used to simulate tumors with defined adjuvanticity and antigenicity conditions. We assumed that these nine phenotypes constitute a wide spectrum of situations that can arise in a solid tumor, which is consistent with previous frameworks of evolutionary-ecological properties of tumors (24).

In silico treatment strategy testing

We simulated the effects of a range of different treatments (details in Supplementary Methods): Chemotherapy (CH) increases the death rate of tumor cells upon proliferation, lymphocyte boost (LB) increases the lymphocyte influx into the domain, anti–Programmed Death 1 treatment (PD) un-exhausts exhausted T lymphocytes and increases the exhaustion tolerance of T lymphocytes as described by Chen and Mellman (25); furthermore, we implemented macrophage repolarization (RE) as described by Halama and colleagues (10), macrophage depletion (MD), stroma permeabilization (SP), and tumor cell migration inhibition (MI) as discussed by Waclaw and colleagues (9). Simulated treatments could be applied in any dose between 0% and 100% and in any combination (except MD that was performed only once). If not otherwise noted, low, medium, and high treatment intensities correspond to 25%, 50%, and 75%, respectively.

Data visualization and statistics

Tumor growth after treatment compared with tumor growth without treatment is visualized in box plots. In each box plot, the central mark indicates the median, the bottom and top edges of the box show the 25th and 75th percentiles. The whiskers extend to the most extreme nonoutlier data points. Outliers are plotted separately as a "+."

Results

The model reproduces cellular composition and architecture of human cancer

During model fitting, we observed that loss function values <1 were easily achieved after few algorithm iterations. As the loss function contained realistic measurements for cellular composition and cellular functional state (see Supplementary Methods), this finding confirmed that the model is able to represent features of human cancer. To test further whether the model also reproduces key aspects of the spatial tissue architecture, we compared the simulated millimeter scale tumors to actual millimeter scale histologic images of human colorectal cancer. Colorectal cancer liver metastases, like most human solid tumors, are not—as previous models assumed (9)—homogenous spheres of cells. Instead, they are characterized by tumor islands and protrusions separated by desmoplastic stroma ridges (Fig. 2A and B), which were also present in our model (Fig. 2C). Similarly, desmoplastic (Fig. 2A) and pushing (Fig. 2B) growth patterns (26) were observed in the simulations (Fig. 2C).

The model predicts OS of human patients with colorectal cancer

To further validate whether the model has a meaningful connection to actual clinical events, we used patient-specific fitting in an independent validation cohort of $N = 24$ patients who had undergone surgical resection of colorectal cancer liver metastases. Based on histologic measurements, we created a parameter vector for each patient and, after patient-specific parameter fitting, assessed *in silico* growth dynamics of the respective simulated tumors. Tumors that showed a faster growth *in silico* (in 12 technical replicates) defined a patient subgroup with shorter OS as compared with slow-growing *in silico* explants ($P < 0.050$, Fig. 2D). To our knowledge, this is the first spatial mechanistic model of human cancer with such prognostic power.

Treatment simulation in heterogeneous tumors

Having established that simulated tumors share key characteristics with actual human tumors, we designed an *in silico* array for treatment testing. Treatment with simulated agents started after 40 days of unperturbed initial growth phase and response was assessed after another 20 more days of simulation (Fig. 3A). As actual tumors are very heterogeneous in terms of tumor and host characteristics (24), we used a range of different tumors for this experiment. In particular, whether tumor cells can be attacked by effector lymphocytes depends on tumor cell characteristics, summarized as antigenicity, and host characteristics, summarized as adjuvanticity (Fig. 3B; refs. 1, 17, 24). We used the modeling platform to find parameter vectors that define tumors with high, medium (mid), and low antigenicity and adjuvanticity, respectively (Fig. 3C). In accordance with prior knowledge, we used a range of different simulated treatments (Fig. 3D). These treatments reshaped tumor phenotypes in diverse ways (Fig. 3E). We assessed treatment responses for three different dose levels (25%, 50%, and 75% of maximum dose, Fig. 3F). Simulated chemotherapy showed a roughly linear dose–response relationship across all treated tumors (Fig. 3D, CH) and control treatment did not change tumor growth in all tumors (Fig. 3D, CTRL). MI had a small but linear effect across all tumors (Fig. 3D, MI). Interestingly, lymphocyte-targeted treatments (LB and lymphocyte reinvigoration by anti-PD1, PD) showed a wide range of responses, ranging from a detrimental effect (hyperprogression) to pronounced responses. Combining chemotherapy (CH) with a LB showed the best median treatment response.

Immunotherapy response depends on tumor and host characteristics

To elucidate these heterogeneous response patterns, we analyzed all tumor–host phenotypes separately (Fig. 4A–I). As expected from empirical evidence (27), low and medium antigenicity tumors tended to have a poor response to immunotherapy (no response to LB in Fig. 4A, C, and F). Interestingly, a strong nonlinear effect was present as medium adjuvanticity tumors showed some response to LB even in low and medium antigenicity settings (Fig. 4B and E). Also, in these cases, adding anti-PD1 to chemotherapy increased treatment response (Fig. 4B and E). In medium antigenicity cases, there was an incremental benefit of adding LB to chemotherapy (CH), although LB alone had only a limited effect (Fig. 4D and E). High antigenicity tumors had the best response to immunotherapy by LB, which was consistently improved by adding anti-PD1 (PD) treatment. Also, this result is in accordance with the literature, as anti-PD1 treatment is widely used to improve action of other immunotherapy approaches (2). All above-mentioned changes were statistically significant after correction for multiple testing (Supplementary Fig. S4A). In our simulation, macrophage-targeted therapy (repolarization agent

Published OnlineFirst July 2, 2018; DOI: 10.1158/0008-5472.CAN-18-1126

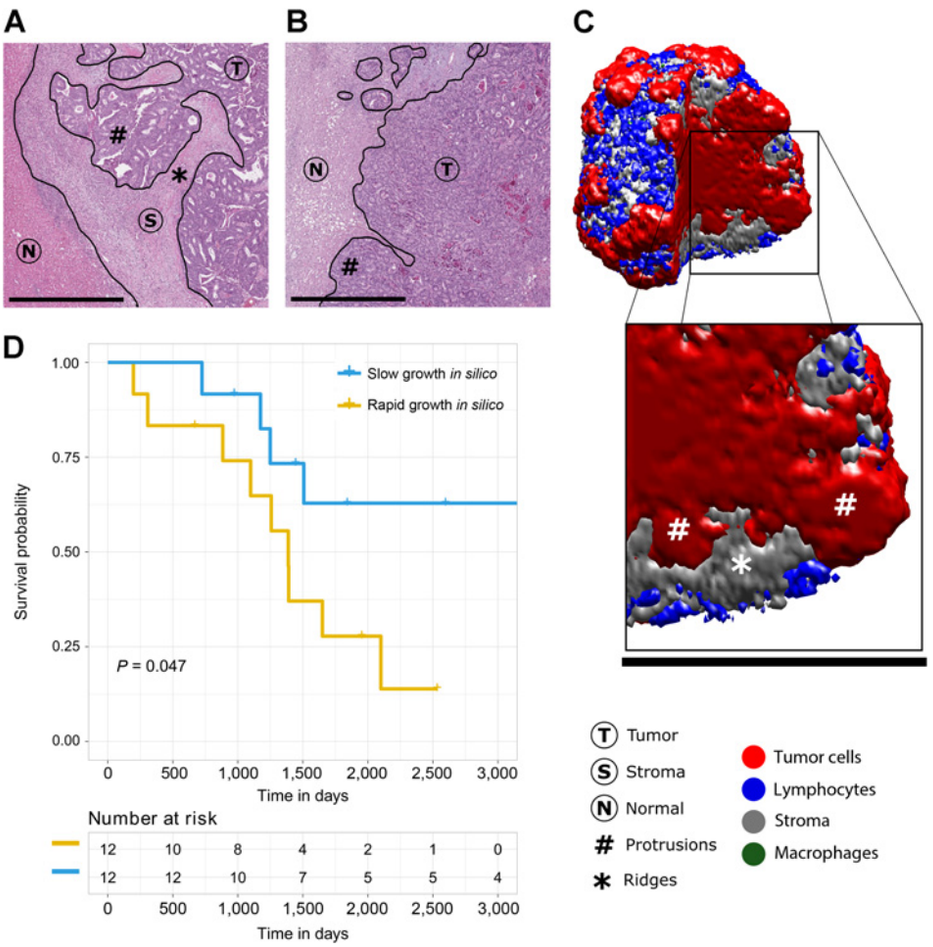

Figure 2.
Histopathologic and clinical validation of the model. **A,** Histologic image of a desmoplastic-type colorectal cancer liver metastasis, showing tumor protrusions and stromal ridges. **B,** Pushing-type colorectal cancer liver metastasis, showing tumor protrusions. **C,** Simulated tumor with a realistic phenotype (loss <1) reflecting these architectural features that were not explicitly built into the model. **D,** OS in a cohort of 24 human patients with colorectal cancer after resection of liver metastases stratified by rapid or slow growth of personalized *in silico* tumor explants (stratification at the median). Rapid growth *in silico* defines a subgroup with significantly worse survival ($P = 0.047$ in log-rank test, which is <0.050). All scale bars are 1 mm.

RE or MD) consistently showed a small additive effect in any tumor–host setting (Supplementary Fig. S4B).

Clinically, it has been previously observed that immunotherapy may in some cases cause tumor hyperprogression, although the exact mechanisms for this effect are unknown (28). Hyperprogressive disease is a speed-up of tumor growth after immunotherapy (28) as opposed to pseudoprogression, which is a type of treatment response with a paradoxical increase in the total tumor volume due to lymphocyte influx. In our model, we count the number of viable tumor cells as opposed to the tumor volume, so we will not observe pseudoprogression. However, we did observe cases of hyperprogression when reinvigorating exhausted T lymphocytes by simulated anti-PD1 treatment (PD), especially in medium antigenicity/medium adjuvanticity settings and in high antigenicity settings (Fig. 4E, H, and I). As described in our previous study (15), we observed a tumor hyperprogression upon treatment with an SP agent (Supplementary Fig. S4C). Interestingly, this effect only occurred in high antigenicity tumors (Supplementary Fig. S4C).

Targeting small-scale cell migration provides additive benefit to other treatments

Inhibiting small-scale migration of tumor cells has been put forward as a therapeutic strategy previously (9), but its relationship to other treatment approaches is unclear. We saw that in our model system, inhibiting tumor cell migration (adding "MI" agent to the system) had no meaningful additive effect to LB in a high antigenicity setting (Fig. 4G-F). However, MI sensitized tumors to LB immunotherapy in two of three medium antigenicity settings (Fig. 4D and F). In most cancer phenotypes, MI had an additive effect to chemotherapy (CH).

Discussion

Previous *in vitro* and *in vivo* models of human solid tumors

Several different approaches for high-throughput drug screening for human solid tumors have been proposed. Thirty years ago, drug screening in cell lines was already used (29) and, over time, modeling systems have gained complexity. Nowadays, *in vitro* systems such as tumor organoids and *in vivo* systems such as PDX models are widely used for preclinical purposes. These models reflect crucial parts of actual human tumors such as genomic makeup and sensitivity to drugs targeting signaling pathways in tumor cells (3, 4, 30). However, there are two major shortcomings of these models that our *in silico* model could address. First, *in vitro* and *in vivo* systems require technical expertise and long hands-on time. Although laboratory automation can help to increase scalability, these models are expensive, not infinitely scalable. This is one of the reasons that currently preclude drug-sensitivity testing in actual clinical settings. Second, prognosis and drug sensitivity

Published OnlineFirst July 2, 2018; DOI: 10.1158/0008-5472.CAN-18-1126

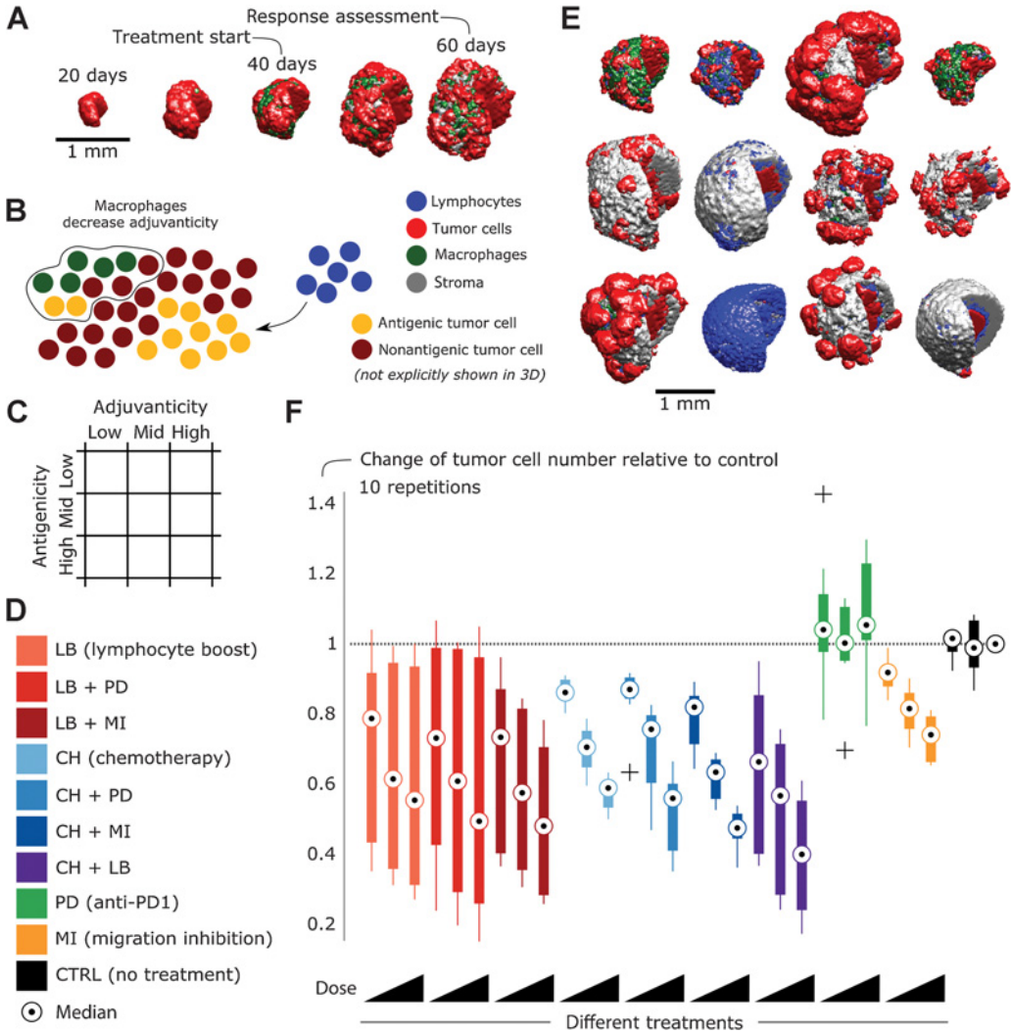

Figure 3.

High-throughput combination immunotherapy drug screening in heterogeneous tumors. **A,** Treatment assessment assay. Simulated treatment is given after 40 days and response is assessed after 60 days. **B,** The model incorporates antigenicity by which tumor cells accumulate mutations and can eventually be attacked by lymphocytes. Also, adjuvanticity is modeled, which is decreased by macrophages, thereby protecting tumor cells in their surroundings from being attacked. **C,** Nine phenotypes of tumors are modeled, ranging from low to high antigenicity and adjuvanticity. **D-F,** Types of treatment used in this experiment (**D**), heterogeneous morphologies of tumor arise after treatment (**E**), and change of tumor cell number 20 days after treatment as a proxy for treatment response for nine different treatment combinations in three dose levels each (25%, 50%, and 75% of maximum dose; **F**). Treatment responses (low/high adjuvanticity/antigenicity) are mixed.

of all solid tumors and particularly colorectal cancer are largely determined by the host immune system. Lymphocytes and macrophages are most imminently interwoven with clinical outcome of colorectal cancer (1). It is not trivial to include these cell types in existing *in vitro* and *in vivo* models. Our *in silico* model aims to fill this gap.

A spatial computational model to complement other *ex vivo* models in colorectal cancer

We use a spatial agent-based approach to model tumor cells, fibrotic stroma, lymphocytes, and macrophages in human metastatic colorectal cancer. In this model, the basic level of abstraction is an individual cell. Thus, all processes on a molecular level are not explicitly taken into account, but only indirectly influence the model as it is based on biological measurements. Although this is a massive simplification and precludes testing of molecularly targeted drugs on a subcellular level, our model accurately recapitulates the emergent behavior on a cellular and tissue level. We assume that although chemotherapy or immunotherapies such as checkpoint inhibitors act on a molecular level, they change cellular behavior and can therefore be investigated using our simulation platform. As our model is specifically adapted to human metastatic colorectal cancer, it includes lymphocytes and macrophages as the two major immune cell types that shape prognosis in this disease (1). In other tumor entities, regulatory T cells (Treg) and myeloid derived suppressor cells also play a

Published OnlineFirst July 2, 2018; DOI: 10.1158/0008-5472.CAN-18-1126

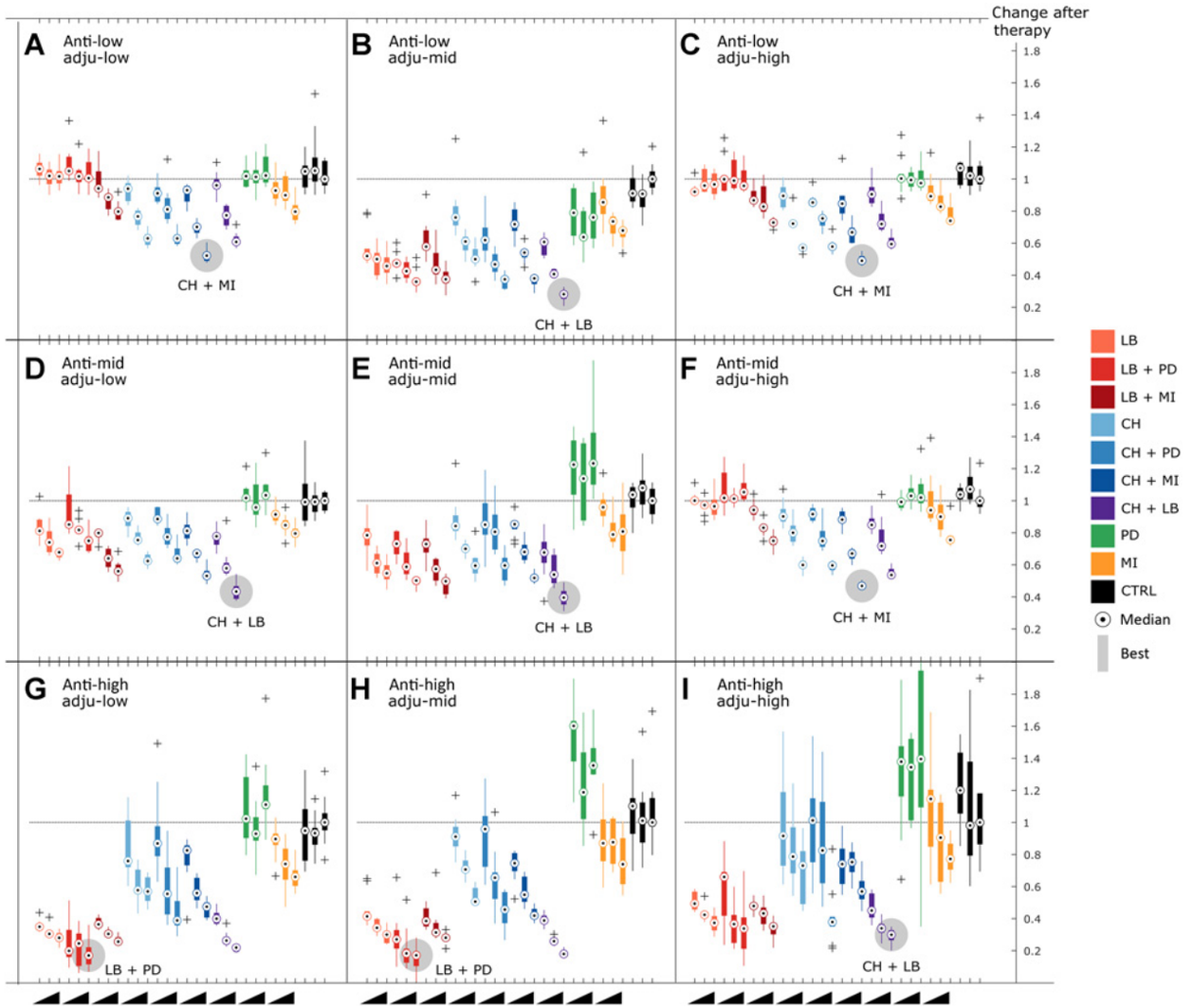

Figure 4.

Prediction of optimal immunotherapy combination depends on tumor and host characteristics. Nine different tumor phenotypes with low/mid/high antigenicity (anti) and low/mid/high adjuvanticity (adju) were simulated and treated with nine different treatments in three different dose levels (25%, 50%, and 75%). These treatments are identical to Fig. 3F but show distinct effects on different tumor phenotypes. Simulated treatments are LB (e.g., by adoptive cell therapy, vaccination, or successful checkpoint blockade), PD (lymphocyte reinvigoration, e.g., by anti-PD1), MI, CH (chemotherapy), and CTRL (control, no treatment). Each experiment included 10 independent repetitions (this figure contains results from 2,700 full model runs). The best treatment in each tumor–host phenotype environment is highlighted in gray and labeled. **A–F,** In low-to-mid antigenicity conditions, CH + MI or CH + PD are optimal. **G–I,** In high antigenicity conditions, LB + PD and CH + PD have the best effect, while PD alone leads to hyperprogression.

major role (31). We release the source code of our model, ensuring that it can easily be adapted to other clinical settings and other tumor entities beyond colorectal cancer liver metastases.

In silico modeling for screening of immunotherapy combination strategies

Previous studies have demonstrated that nonspatial (32, 33) and spatial (9, 14, 15, 34–36) mechanistic models of human solid tumors are very useful tools and complement classical laboratory models for cancer research. However, to our knowledge, there is currently no mechanistic spatial model of solid tumor tissue that can predict prognosis and can be used to screen new combination treatment strategies. We show for a clinically highly relevant scenario that our spatial model represents key aspects of tumor morphology, can stratify patients and predict prognosis, and can be used to test treatment strategies in different tumor–host settings.

We investigate various combinations of simulated treatments: Chemotherapy (CH) induces tumor cell death upon proliferation; LB increases the lymphocyte influx into the domain; lymphocyte reinvigoration (PD) turns exhausted lymphocytes into active lymphocytes and prevents their exhaustion and MI reduces the migration probability of tumor cells. *In vivo* studies have shown that the effect of checkpoint inhibitors such as anti-PD1

Published OnlineFirst July 2, 2018; DOI: 10.1158/0008-5472.CAN-18-1126

reinvigorate exhausted lymphocytes (25) but they also profoundly change the tumor microenvironment and increase T-lymphocyte numbers in the tumor (37). Beyond anti-PD1, LB also encompasses effects of adoptive T-cell therapy, vaccination, and anti-CTLA4 therapy, all of which aim to increase the number of activated T cells in the tumor microenvironment. In contrast to other preclinical model systems, our computer-based simulation can actually analyze un-exhaustion (PD) and lymphocyte increase (LB) independently of each other. Interestingly, we observe that un-exhaustion alone (PD, as put forward previously; ref. 25) does not result in tumor regression in any tumor phenotype (Fig. 4A–I). However, combining un-exhaustion with increased lymphocyte influx does have a synergistic effect in a high antigenicity setting (Fig. 4G–I). This is consistent with experimental findings showing that responders to anti-PD1 therapy experience a pronounced increase in lymphocyte numbers in their tumors (37). Thus, our model recapitulates key aspects of experimental findings on how the tumor microenvironment shapes immunotherapy response, while allowing much more control about the actual processes than other *in vitro* or *in vivo* model platforms.

Personalized recommendations for combination immunotherapy in colorectal cancer

We show that optimal responses in different tumor phenotypes are achieved by different combination therapies. These tumor phenotypes differed in terms of antigenicity and adjuvanticity, two major evolutionary-ecological determinants of tumor–immune interactions (1, 17, 24). To date, this concept has not yet been tested in the clinic. However, our results suggest that by using already established biomarkers such as mutational load as a proxy for antigenicity and macrophage abundance (and possibly other immunosuppressive factors such as stromal abundance, TGF-beta levels (38) or macrophage abundance and polarization status) as a proxy for adjuvanticity, personalized treatment recommendations could be made. Our model can be calibrated in a patient-specific way by using immunohistochemical data. Thus, it can be easily incorporated into clinical trials for prospective validation.

Disclosure of Potential Conflicts of Interest

No potential conflicts of interest were disclosed.

Authors' Contributions

Conception and design: J.N. Kather, M. Suarez-Carmona, F. Klupp, J. Poleszczuk, N. Halama
Development of methodology: J.N. Kather, J. Poleszczuk
Acquisition of data (provided animals, acquired and managed patients, provided facilities, etc.): J.N. Kather, P. Charoentong, M. Suarez-Carmona, E. Herpel, F. Klupp, M. Schneider, N. Halama
Analysis and interpretation of data (e.g., statistical analysis, biostatistics, computational analysis): J.N. Kather, D. Jaeger, N. Halama
Writing, review, and/or revision of the manuscript: J.N. Kather, M. Suarez-Carmona, F. Klupp, A. Ulrich, M. Schneider, I. Zoernig, T. Luedde, D. Jaeger, J. Poleszczuk, N. Halama
Administrative, technical, or material support (i.e., reporting or organizing data, constructing databases): E. Herpel, F. Klupp, I. Zoernig, D. Jaeger, N. Halama
Study supervision: I. Zoernig, J. Poleszczuk, N. Halama

Acknowledgments

The authors would like to thank Anita Heinzelmann, Rosa Eurich, and Jana Wolf (National Center for Tumor Diseases, Heidelberg, Germany), Katrin Wolk (University Medical Center Mannheim, Mannheim, Germany), and Nina Wilhelm (NCT Biobank, National Center for Tumor diseases, Heidelberg, Germany) for expert technical assistance. The authors are very grateful to Dr. Charles Neu (University Hospital Jena, Jena, Germany) for proofreading the article. Tissue samples for this study were provided by the tissue bank of the National Center for Tumor Diseases (NCT, Heidelberg, Germany). The results shown here are in part based upon data generated by the TCGA Research Network: http://cancergenome.nih.gov/. We gratefully acknowledge the support of NVIDIA Corporation with the donation of a Titan Xp GPU used for this research (granted to J.N. Kather).

J.N. Kather is supported by the "Heidelberg School of Oncology" (NCT-HSO) and by the "German Consortium for Translational Cancer Research" (DKTK) fellowship program.

The costs of publication of this article were defrayed in part by the payment of page charges. This article must therefore be hereby marked *advertisement* in accordance with 18 U.S.C. Section 1734 solely to indicate this fact.

Received April 13, 2018; revised May 24, 2018; accepted June 26, 2018; published first July 2, 2018.

References

1. Kather JN, Halama N, Jaeger D. Genomics and emerging biomarkers for immunotherapy of colorectal cancer. Semin Cancer Biol 2018. pii: S1044-579X(17)30254-7. doi: 10.1016/j.semcancer.2018.02.010.
2. Kather JN, Berghoff AS, Ferber D, Suarez-Carmona M, Reyes-Aldasoro CC, Valous NA, et al. Large-scale database mining reveals hidden trends and future directions for cancer immunotherapy. OncoImmunology 2018: e1444412:1–23.
3. van de Wetering M, Francies HE, Francis JM, Bounova G, Iorio F, Pronk A, et al. Prospective derivation of a living organoid biobank of colorectal cancer patients. Cell 2015;161:933–45.
4. Hidalgo M, Amant F, Biankin AV, Budinska E, Byrne AT, Caldas C, et al. Patient-derived xenograft models: an emerging platform for translational cancer research. Cancer Discov 2014;4:998–1013.
5. Kopetz S, Lemos R, Powis G. The promise of patient-derived xenografts: the best laid plans of mice and men. Clin Cancer Res 2012;18:5160–2.
6. Gao H, Korn JM, Ferretti S, Monahan JE, Wang Y, Singh M, et al. High-throughput screening using patient-derived tumor xenografts to predict clinical trial drug response. Nat Med 2015;21:1318.
7. Karolak A, Markov DA, McCawley LJ, Rejniak KA. Towards personalized computational oncology: from spatial models of tumour spheroids, to organoids, to tissues. J R Soc Interface 2018;15.pii:20170703.
8. Letort G, Montagud A, Stoll G, Heiland R, Barillot E, Macklin P, et al. PhysiBoSS: a multi-scale agent based modelling framework integrating physical dimension and cell signalling. bioRxiv 2018. doi: https://doi.org/10.1101/267070
9. Waclaw B, Bozic I, Pittman ME, Hruban RH, Vogelstein B, Nowak MA. A spatial model predicts that dispersal and cell turnover limit intratumour heterogeneity. Nature 2015;525:261–4.
10. Halama N, Zoernig I, Berthel A, Kahlert C, Klupp F, Suarez-Carmona M, et al. Tumoral immune cell exploitation in colorectal cancer metastases can be targeted effectively by anti-CCR5 therapy in cancer patients. Cancer Cell 2016;29:587–601.
11. Ghaffarizadeh A, Heiland R, Friedman SH, Mumenthaler SM, Macklin P. PhysiCell: an open source physics-based cell simulator for 3-D multicellular systems. PLoS Comput Biol 2018;14:e1005991.
12. Bankhead P, Fernandez JA, McArt DG, Boyle DP, Li G, Loughrey MB, et al. Integrated tumor identification and automated scoring minimizes pathologist involvement and provides new insights to key biomarkers in breast cancer. Lab Invest 2018;98:15–26.
13. Bankhead P, Loughrey MB, Fernandez JA, Dombrowski Y, McArt DG, Dunne PD, et al. QuPath: Open source software for digital pathology image analysis. Sci Rep 2017;7:16878.
14. Poleszczuk J, Macklin P, Enderling H. Agent-Based Modeling of Cancer Stem Cell Driven Solid Tumor Growth. Methods Mol Biol 2016;1516:335–46.
15. Kather JN, Poleszczuk J, Suarez-Carmona M, Krisam J, Charoentong P, Valous NA, et al. *In silico* modeling of immunotherapy and stroma-

targeting therapies in human colorectal cancer. Cancer Res 2017;77:6442–52.
16. Koelzer VH, Canonica K, Dawson H, Sokol L, Karamitopoulou-Diamantis E, Lugli A, et al. Phenotyping of tumor-associated macrophages in colorectal cancer: Impact on single cell invasion (tumor budding) and clinicopathological outcome. Oncoimmunology 2016;5:e1106677.
17. Galluzzi L, Buque A, Kepp O, Zitvogel L, Kroemer G. Immunogenic cell death in cancer and infectious disease. Nat Rev Immunol 2017;17:97–111.
18. McGranahan N, Furness AJ, Rosenthal R, Ramskov S, Lyngaa R, Saini SK, et al. Clonal neoantigens elicit T cell immunoreactivity and sensitivity to immune checkpoint blockade. Science 2016;351:1463–9.
19. Luksza M, Riaz N, Makarov V, Balachandran VP, Hellmann MD, Solovyov A, et al. A neoantigen fitness model predicts tumour response to checkpoint blockade immunotherapy. Nature 2017;551:517–20.
20. Efremova M, Rieder D, Klepsch V, Charoentong P, Finotello F, Hackl H, et al. Targeting immune checkpoints potentiates immunoediting and changes the dynamics of tumor evolution. Nat Commun 2018;9:32.
21. Wu X, Zhang H, Xing Q, Cui J, Li J, Li Y, et al. PD-1(+) CD8(+) T cells are exhausted in tumours and functional in draining lymph nodes of colorectal cancer patients. Br J Cancer 2014;111:1391–9.
22. de Sousa e Melo F, Kurtova AV, Harnoss JM, Kljavin N, Hoeck JD, Hung J, et al. A distinct role for Lgr5(+) stem cells in primary and metastatic colon cancer. Nature 2017;543:676–80.
23. Halama N, Michel S, Kloor M, Zoernig I, Benner A, Spille A, et al. Localization and density of immune cells in the invasive margin of human colorectal cancer liver metastases are prognostic for response to chemotherapy. Cancer Res 2011;71:5670–7.
24. Maley CC, Aktipis A, Graham TA, Sottoriva A, Boddy AM, Janiszewska M, et al. Classifying the evolutionary and ecological features of neoplasms. Nat Rev Cancer 2017;17:605–19.
25. Chen DS, Mellman I. Elements of cancer immunity and the cancer-immune set point. Nature 2017;541:321–30.
26. van Dam PJ, van der Stok EP, Teuwen LA, Van den Eynden GG, Illemann M, Frentzas S, et al. International consensus guidelines for scoring the histopathological growth patterns of liver metastasis. Br J Cancer 2017;117:1427–41.
27. Le DT, Uram JN, Wang H, Bartlett BR, Kemberling H, Eyring AD, et al. PD-1 blockade in tumors with mismatch-repair deficiency. N Engl J Med 2015;372:2509–20.
28. Champiat S, Dercle L, Ammari S, Massard C, Hollebecque A, Postel-Vinay S, et al. Hyperprogressive disease is a new pattern of progression in cancer patients treated by anti-PD-1/PD-L1. Clin Cancer Res 2017;23:1920–8.
29. Alley MC, Scudiero DA, Monks A, Hursey ML, Czerwinski MJ, Fine DL, et al. Feasibility of drug screening with panels of human tumor cell lines using a microculture tetrazolium assay. Cancer Res 1988;48:589–601.
30. Vlachogiannis G, Hedayat S, Vatsiou A, Jamin Y, Fernández-Mateos J, Khan K, et al. Patient-derived organoids model treatment response of metastatic gastrointestinal cancers. Science 2018;359:920–6.
31. Vinay DS, Ryan EP, Pawelec G, Talib WH, Stagg J, Elkord E, et al. Immune evasion in cancer: mechanistic basis and therapeutic strategies. Semin Cancer Biol 2015;35Suppl:S185–S98.
32. Kuznetsov VA, Makalkin IA, Taylor MA, Perelson AS. Nonlinear dynamics of immunogenic tumors: parameter estimation and global bifurcation analysis. Bull Math Biol 1994;56:295–321.
33. Gatenby RA, Silva AS, Gillies RJ, Frieden BR. Adaptive therapy. Cancer Res 2009;69:4894–903.
34. Sottoriva A, Kang H, Ma Z, Graham TA, Salomon MP, Zhao J, et al. A Big Bang model of human colorectal tumor growth. Nat Genet 2015;47:209–16.
35. Anderson AR, Weaver AM, Cummings PT, Quaranta V. Tumor morphology and phenotypic evolution driven by selective pressure from the microenvironment. Cell 2006;127:905–15.
36. Enderling H, Anderson AR, Chaplain MA, Beheshti A, Hlatky L, Hahnfeldt P. Paradoxical dependencies of tumor dormancy and progression on basic cell kinetics. Cancer Res 2009;69:8814–21.
37. Riaz N, Havel JJ, Makarov V, Desrichard A, Urba WJ, Sims JS, et al. Tumor and microenvironment evolution during immunotherapy with nivolumab. Cell 2017;171:934–49e15.
38. Tauriello DVF, Palomo-Ponce S, Stork D, Berenguer-Llergo A, Badia-Ramentol J, Iglesias M, et al. TGFbeta drives immune evasion in genetically reconstituted colon cancer metastasis. Nature 2018;554:538–43.

Published OnlineFirst July 2, 2018; DOI: 10.1158/0008-5472.CAN-18-1126

Cancer Research
The Journal of Cancer Research (1916–1930) | The American Journal of Cancer (1931–1940)

AACR American Association for Cancer Research

High-Throughput Screening of Combinatorial Immunotherapies with Patient-Specific *In Silico* Models of Metastatic Colorectal Cancer

Jakob Nikolas Kather, Pornpimol Charoentong, Meggy Suarez-Carmona, et al.

Cancer Res 2018;78:5155-5163. Published OnlineFirst July 2, 2018.